

High Voltage Amplifier Designs for Penning and Radio-Frequency Traps

B. T. Chang and T. B. Mitchell

Department of Physics and Astronomy, University of Delaware, Newark, Delaware, 19716

Abstract. Two economical designs for high voltage amplifiers are described, and the performance of constructed units is characterized. The first amplifier is based on a design originating from the non-neutral plasma group at UC San Diego, and is useful for driving capacitive loads such as the containment rings of Penning traps. The second is based on a design published by the Jones group of the University of Utah Chemistry Department, and is designed to power radio-frequency (rf) guides and traps. Complete design specifications including schematics, PC board files and circuit simulation inputs are available for those interested in building either amplifier [1].

Charged-particle traps require confinement fields in order to provide potential wells. In this contribution we describe two economical solutions for providing electric fields for use with Penning and radio-frequency (rf) traps.

With Penning traps, radial confinement is provided by an axial magnetic field while axial confinement is provided by electric fields. In a typical electron plasma experiment, large voltage amplitudes of ~ 100 V applied to trap electrodes are needed to provide confinement of electrons with densities of $\sim 10^7 \text{cm}^{-3}$ and length ~ 20 cm [2]. The voltage waveforms should be readily adjustable to permit fine control of the injection process [3] and later shaping of the electron distribution [4, 5]. The bandwidth of the amplifier should be as wide as possible to permit fast density measurements [6]. Total harmonic distortion should be minimized to allow the amplifier to be used to apply large perturbations such as can be needed for rotating wall frequency stabilization [7]. These requirements can be met with a DC-coupled high voltage amplifier with a gain of 15 (to allow control with computer-controlled DAQ cards with ± 10 V outputs).

With rf traps, an oscillator modulates the potential applied to a trap electrode(s) at typical frequencies of 1 MHz and greater, and amplitudes of $20 V_{p-p}$ to $900 V_{p-p}$. The time-dependent electric field can result in a pondermotive force which, depending on amplitude and frequency, will trap particles of particular charge to mass (q/m) ratios while ejecting others [8]. The ideal rf oscillator can be switched off rapidly (to facilitate ion ejection), is stable and tunable in both frequency and amplitude, and is well coupled to the trap.

High Voltage DC-Coupled Amplifier

Our high voltage amplifier design utilizes the Apex PA84A high voltage power operational amplifier, and is based on a circuit designed by Bob Bongard of UCSD. The

amplifier accepts up to ± 9.5 V input, has a voltage gain of -15, can output $\sim \pm 25$ mA, and has a 2000Ω input impedance. It is designed to drive a capacitive load C_L on the order of ~ 300 pF. The difficult aspect of the circuit design is accomplishing this while avoiding oscillations. The method used is to avoid poles in the characteristic polynomial of the closed loop transfer function, and to introduce zeros to cancel unavoidable ones.

The current limits of the op-amp limit the maximum slew rate possible. A $1\text{ k}\Omega$ output isolation resistor R_{iso} creates a zero to eliminate a pole caused by the internal PA84A output resistance and the capacitive load. This $R_{iso}-C_L$ network establishes the slew rate and the bandwidth (as measured by the frequency at which the output is 3 dB down). With no load and maximum output amplitude, the amplifier slew rate is $245\text{ V}/\mu\text{s}$ and its bandwidth is 320 kHz. These figures reduce linearly with load capacitance, and are $135\text{ V}/\mu\text{s}$ and 185 kHz with a load of 500 pF.

The amplifier's total harmonic distortion (THD) is roughly independent of the load capacitance, but increases with frequency. We characterized the performance by driving the amplifier with a sinusoidal input with a THD of 0.35%, and measuring the THD of the output with an amplitude near the maximum value achievable of 270 V_{p-p} . At 20 Hz, the output was similar to the input with a THD of $\sim 0.30\%$, but at 50 kHz we measured THD $\sim 0.70\%$.

In the full version of the amplifier, analog switches, potentiometers and op amps are used in the front end along with panel mounted controls to provide a great deal of flexibility for pulse generation. TTL voltage levels are used to select one of two inputs for the amplifier, either of which can be supplied by either external signals or user-controlled DC levels. These advanced features can be bypassed by a jumper to provide a simplified amplifier with a single input.

Complete design specifications are available at [1]. This website includes Gerber 274X images and Excellon drill files which can be used to fabricate a two-layer fiberglass printed circuit board. It also includes CAD drawings for the amplifier housing, electronic schematic diagram files, PC board design files and some SPICE models. (The parts of the circuit for which SPICE models were available were simulated in Electronics Workbench's Multisim 2001 to verify that the circuit would work.) An accompanying parts lists indicates suggested vendors and costs of components. One full amplifier costs about \$600 to build. Simplified amplifiers use the same board but require fewer components and cost about \$450.

Although the amplifier circuit is intended to benefit from the application of negative feedback, every attempt has been made to eliminate sources of positive feedback, which can result in uncontrollable oscillations. Potential sources of positive feedback include modulation on DC supply lines that is coupled back into the amplifier, non-zero ground voltages reaching the non-inverting amplifier input which is also grounded, near 360° phase shift at unity loop gain, parasitic capacitance on the op amp input which must be compensated, and improper placement of feedback components and paths near high amplitude signals and ground returns.

Radio Frequency High Voltage Amplifier

In this section we describe the design of a high voltage 2.50 MHz frequency rf oscillator capable of sinusoidal output with linear amplitude controllable from 100 V_{pp} to 900 V_{pp} . It can be switched off from a 6146 vacuum tube anode voltage of 900 V_{pp} to 0 V_{pp} in 30 nanoseconds. It is intended for use with an ion trap for trapping and time-of-flight experiments. Because the ion trap serves as a capacitive load that participates in an inductor-capacitor tank of the rf oscillator, no impedance matching transformer is needed.

The basic oscillator design is motivated by the work of the Jones group of the University of Utah Chemistry department [9, 10, 11]. Two 6146 vacuum tubes are connected in an astable multivibrator configuration, with the output anode of each tube driving the grid input of the other tube. With a parallel LC tank circuit connected between the two anodes, the circuit never comes to rest in a stable configuration, and instead freely oscillates. The frequency of oscillation is fixed, but can be adjusted from a few hundreds kHz to about 25 MHz by changing the inductance of the tank circuit.

Based upon recommended gains, current and voltage levels in data sheets for 6146 tubes used as rf oscillators, and upon Jones' circuit designs [11], we constructed a prototype oscillator but encountered parasitic oscillations when we sought to improve the amplitude and frequency stability. To investigate these, we used Electronic Workbench's Multisim 2001 circuit modelling software package. This software accurately predicted that the resonant frequency of the rf oscillator would be the measured value of $\omega_0 = 1.57 \cdot 10^7$ rad/sec, and be sensitive to mutual reflected impedance between the halves of the tank inductor, with the center-tap capacitively bypassed to ground. (Although seemingly each tube drives a parallel LC circuit of a 15 μ H inductor half and a 131pF 4.1 ft. cable with grounded braided shield from its anode and ground, the reflected mutual impedance of $M = 11.55 \mu$ H affects the current flow in the other half of the inductor, as well.)

We then wrote a second software simulation to gain insight into the feedback nature of the circuit, after the working design had been attained. Wolfram Research Inc.'s Control Systems Professional and Mathematica 5.0 software packages were used to translate a set of Kirchoff current and voltage law equations, applying the non-conventional two-loop positive feedback in astable multivibrators to them, to derive state space representations of the circuit. The software translated this into a frequency response which shed light on how the circuit equalizes its effort to minimize energy dissipated in the 6146 plate resistance, while maximizing the current flowing into the tank capacitance, as it ought to at resonance.

Bode plots from the second simulation giving magnitude (Fig. 1) and phase (Fig. 2) of the rf oscillator of the anode 1 voltage, divided by the component of anode 1 current furnished by the DC power supply, show that the transfer function has high gain and, counterintuitively, that the supply does not deliver current to the tube zero degrees out of phase to the voltage, but rather that the voltage lags the supply current by 1.6 degrees at resonance.

At the resonant frequency ω_0 , we found that the anode current and the voltage were out of phase due to a lag effect created by a 313pF capacitance and the 20K Ω plate resistance. A mathematical model found a current flowing **out** of the plate resistor equal

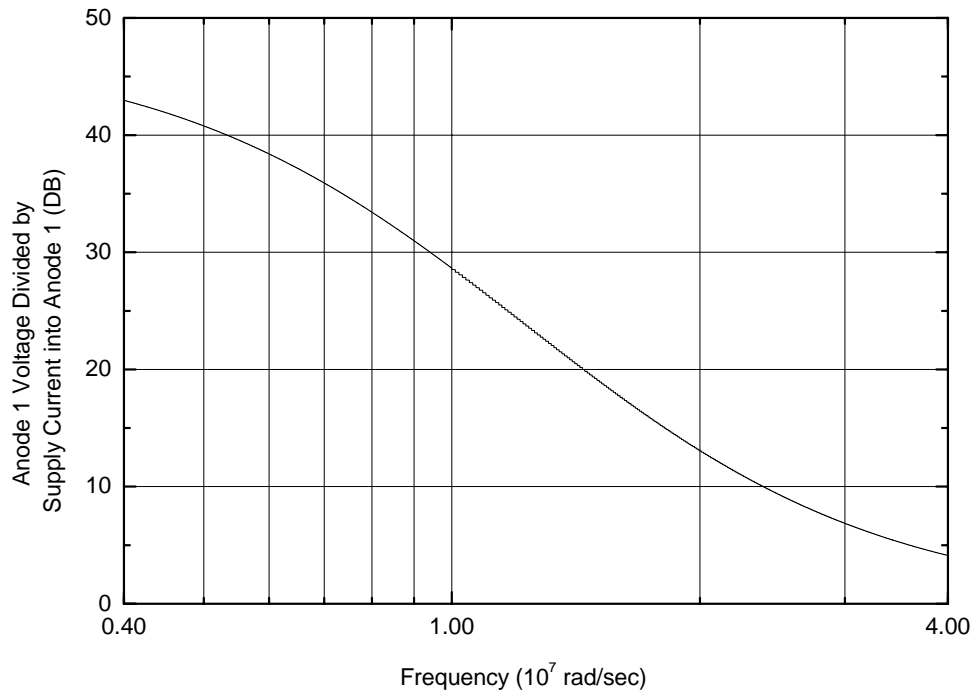


FIGURE 1. Bode plot of the magnitude of the transfer function relating rf oscillator Anode-1 voltage divided by the component of anode 1 current furnished by the DC power supply.

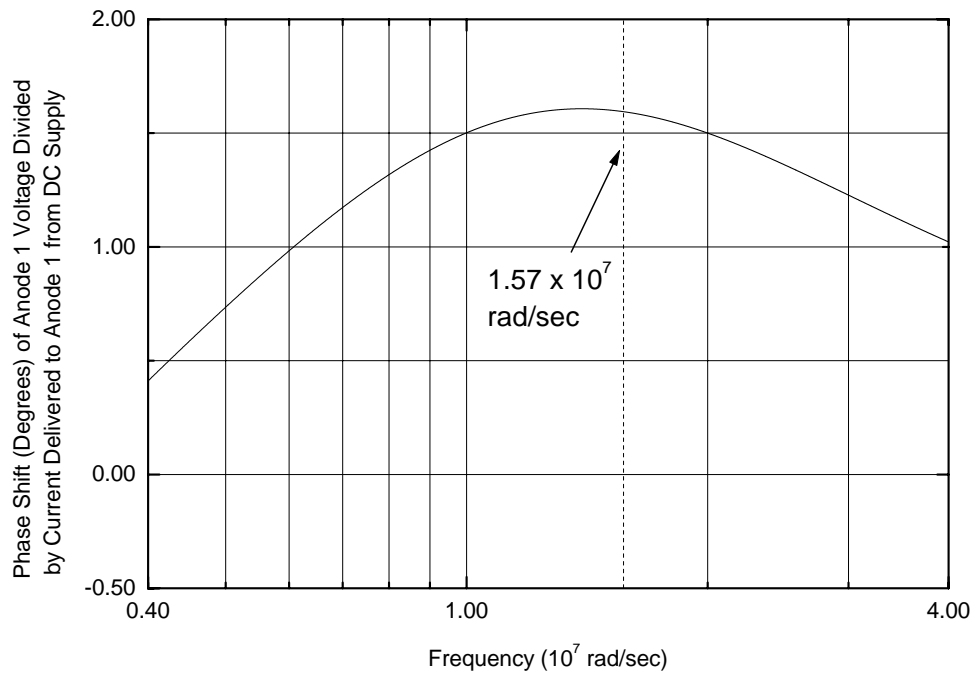


FIGURE 2. Bode plot of the number of degrees the V_{A1} leads the component of anode 1 current furnished by the DC power supply. Positive angles imply V_{A1} leads the current.

to $V_{A1}(2.749 \cdot 10^{-3} \cos(\omega_0 t - 0.02834))$, where V_{A1} is the anode voltage amplitude. A current $V_{A1}(27.7 \cdot 10^{-6} \cos(\omega_0 t + 0.0279))$ flows from the DC supply **into** the resistor. The phases and directions are such that the DC supply furnishes a current whose real part minimizes that of the current in the resistor due to the tube, minimizing the energy lost in it. The imaginary part of current flowing out of the resistor is maximized. It flows into the capacitor, the correct destination for resonant current.

For harmonics other than the ω_0 , the tank becomes heavily inductive, forcing the the current from the power supply to lead the anode voltage. This reduces the phase angle, as seen in Fig. 2.

In the remainder of this contribution, we discuss some changes we have made to the Jones oscillator design.

Noise Reduction The harmonic-content power dissipated in the non-ideal resistance of the tank inductor can be reduced by mixing in a sinusoidal signal having one pure frequency. Phase-different voltages will cancel, and the spectral purity of the output will improve. The mixing was accomplished by adding a **B** field by driving a current into two loops of AWG 22 wire wrapped around one half of the center-tapped tank inductor. A relative clean function-generator-derived 2.5MHz oscillating current of 100 mA_{p-p} was produced using an emitter-follower high current transistor. The improvement from this mixing can be seen in Fig. 3, where the top shows an FFT of the frequency stabilized oscillator's fundamental and first harmonic, and the bottom shows an FFT of a freely running oscillator.

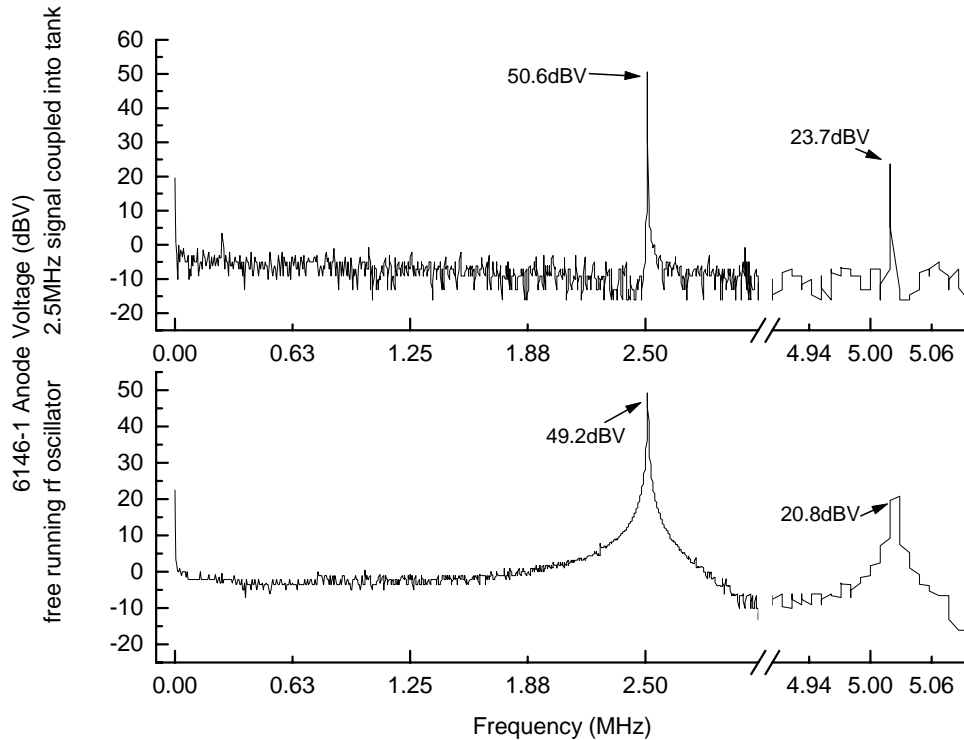


FIGURE 3. Fourier spectrum of the rf oscillator output; freely running (bottom) and stabilized by a 2.50 MHz source (top).

Amplitude control Incorporating a design from Ref. [12], we have added an automatic gain control circuit which provide a linear control of a single anode's voltage in the $100 V_{pp}$ to $900 V_{pp}$ range. Amplitudes from $22 V_{pp}$ to $100 V_{pp}$ range are also attainable, but are not proportional to the control voltage.

We control anode amplitudes by varying the 6146 gains; namely, their grid-cathode voltage dependent transconductance. This is done by varying the cathode current, which then controls the grid-cathode DC bias and also the excursion range of plate-cathode voltages.

To regulate current, a power transistor is connected between the cathode and ground of each tube. Their resistances are variable, and increase to limit current flow. When the the transistors are nearly turned off, corresponding to a small anode voltage output range, the cathodes of the tubes are pulled high. Effectively, the voltage divider pulls the cathode high with a low plate-cathode resistance, while the cathode-ground resistance due to the transistor is very high. This also decreases grid-cathode bias, reducing the gain of the tubes. When the transistors allow strong current flow, their resistance is low, and the cathode-plate potential has a wide range. Grid-cathode voltage is made more positive by a less positive grid. This increases the tube amplification.

Fast turn-off The rf oscillator can be switched on and off rapidly. When shut off, it ramps to zero volts in 30 nanoseconds. We use International Rectifier IR2213 combination high side and low side driver integrated circuit, and IRFPG50 high voltage, high current MOSFET transistors. We use four of the MOSFETs as on-off switches of very large voltages, controlled by small levels.

The high side driver is needed to apply a large voltage to the gates of a MOSFET, supplying or denying high $475V_{DC}$ voltages to our load, the DC power supply line of the rf oscillator. The low side driver grounds this line rapidly when needed.

We use a third and fourth IRFPG50, each connected to a 6146 tube, with their drain connected to the anode, and their source to the ground. When the TTL control is low this second pair conducts, discharging the tubes and the tank circuit and shutting down the oscillations. When the TTL control goes high, this second pair opens.

A very fast high voltage diode, reverse-connected across the DC power supply line is essential to clip turn-off noise transients to levels which would not trigger the oscillator spuriously. These transients are evident in Fig. 4 which plots the control and output voltages during the time turn-off occurs. The figure indicates the sudden turn-off achievable as well as the relative cleanliness of the output.

ACKNOWLEDGMENTS

This research was supported by the National Science Foundation. We wish to thank T. Pham for software assistance, G. Robinson and L. Shulman for analog design tips, J. Poirier for technical assistance, C. F. Driscoll for sharing his group's amplifier design, and D. Schaeffer for constructing amplifiers and measuring their performance.

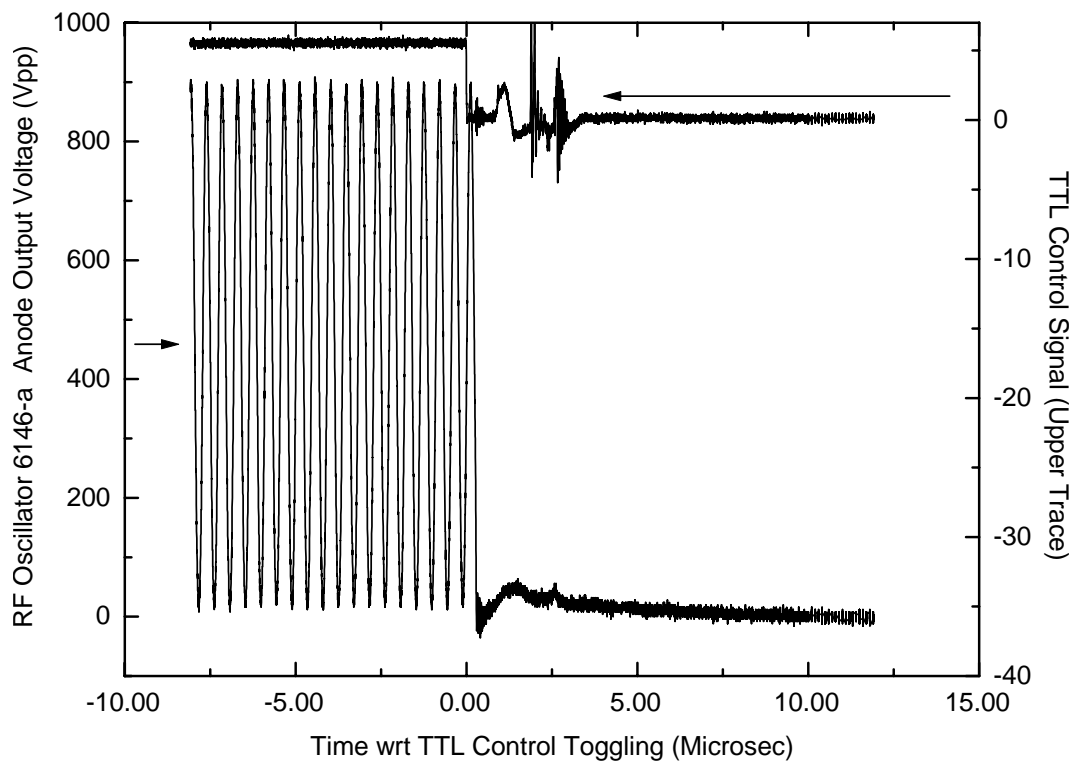


FIGURE 4. Input TTL control signal and oscillator output at turn-off. Note the noise due to inductive kickback and the sudden 900 V transition in 30 nanosec.

REFERENCES

1. www.physics.udel.edu/~mitchell/projects.
2. Prasad, S. A., and O'Neil, T. M., *Phys. Fluids*, **22**, 278 (1978).
3. Kriesel, J. M., and Driscoll, C. F., *Phys. Plasmas*, **5**, 1265–1272 (1998).
4. Driscoll, C. F., *Phys. Rev. Lett.*, **64**, 1528–1543 (1990).
5. Fine, K. S., Driscoll, C. F., Malmberg, J. H., and Mitchell, T. B., *Phys. Rev. Lett.*, **67**, 588 (1991).
6. Malmberg, J. H., and Driscoll, C. F., *Phys. Rev. Lett.*, **44**, 654–657 (1980).
7. Huang, X.-P., Bollinger, J. J., Mitchell, T. B., and Itano, W. M., *Phys. Rev. Lett.*, **80**, 73–76 (1998).
8. Ghosh, P. K., *Ion Traps*, Clarendon, Oxford, 1995.
9. Jones, R. M., Gerlich, D., and Anderson, S. L., *Rev. Sci. Instrum.*, **68**, 3357 (1997).
10. Jones, R. M., and Anderson, S. L., *Rev. Sci. Instrum.*, **71**, 4335 (2000).
11. www.chem.utah.edu/chemistry/staff/jones/rfgen.
12. O'Connor, P. B., Costello, C. E., and Earle, W. E., *J. Am. Soc. Mass Spectrom.*, **13**, 1370 (2002).